

# Study of $\gamma\pi\rightarrow\pi\pi$ below 1 GeV using an integral equation approach

Tran N. Truong

*Centre de Physique Théorique, Ecole Polytechnique F91128 Palaiseau, France  
and Institute of Particle and Nuclear Studies, High Energy Accelerator Research Organization,  
1-1 Oho, Tsukuba, Ibaraki,  
305-0801 Japan*

(Received 16 May 2001; published 30 January 2002)

The scattering of  $\gamma\pi\rightarrow\pi\pi$  is studied using the axial anomaly, elastic unitarity, analyticity, and crossing symmetry. Using the technique to derive Roy's equation, an integral equation for the  $P$ -wave amplitude is obtained in terms of the strong  $P$ -wave pion-pion phase shifts. Its solution is obtained numerically by an iteration procedure using as the starting point the solution of an integral equation of Muskhelishvili-Omnès type. It is, however, ambiguous and depends sensitively on the second derivative of the  $P$ -wave amplitude at  $s=m_\pi^2$  which cannot be directly measured.

DOI: 10.1103/PhysRevD.65.056004

PACS number(s): 11.30.Rd, 11.55.Fv, 11.55.Hx, 13.60.Le

## I. INTRODUCTION

One of the fundamental calculations in particle theory is the  $\pi^0\rightarrow\gamma\gamma$  decay rate [1]. It is a combination of partially conserved axial vector current and the short distance behavior of quantum chromodynamics (QCD):

$$A(\pi^0\rightarrow\gamma\gamma)=iF_{\gamma\gamma}\epsilon^{\mu\nu\sigma\tau}\epsilon_\mu^*k_\nu\epsilon_\sigma^*k'_\tau \quad (1)$$

with

$$F_{\gamma\gamma}=\frac{e^2N_c}{12\pi^2f_\pi}=0.025\text{ GeV}^{-1}, \quad (2)$$

where  $e$  is the electric charge,  $f_\pi=0.0924$  GeV, and  $N_c=3$  is the number of colors in QCD. This calculation is valid in a world where  $\pi^0$  is massless. Some corrections have to be made in order to take into account the finite value of the pion mass. It turns out that the massless pion anomaly formula is in very good agreement with the pion lifetime data [2], implying that the correction due to the physical pion mass in Eq. (2) is very small.

Another axial anomaly result is the process  $\gamma\pi\rightarrow\pi\pi$  or its analytical continuation  $\gamma\rightarrow 3\pi$  [3]. This last process requires more corrections because, for practical considerations, measurements are done at an energy far from the chiral limit where the anomaly formula is applicable. Furthermore, the analytical continuation from one process to the other is a delicate procedure due to the presence of a complex singularity, which is absent in the former reaction. The calculation of the process  $\gamma\pi\rightarrow\pi\pi$  is in itself interesting because of future experiments being proposed at various accelerator facilities and also its important role in the calculation of  $\pi^0\rightarrow\gamma\gamma^*$  [4].

The  $\gamma\pi\rightarrow\pi\pi$  amplitude is given by

$$\begin{aligned} A(\gamma(k)\pi^0(p_0)\rightarrow\pi^+(p_1)\pi^-(p_2)) \\ =i\epsilon^{\mu\nu\sigma\tau}\epsilon_\mu p_{0\nu}p_{1\sigma}p_{2\tau}G(s,t,u) \end{aligned} \quad (3)$$

where  $s$ ,  $t$ , and  $u$  are the kinematical variables for this process and will be defined below. In the chiral limit (the zero limit of the pion four-momenta), the matrix element is given by the anomaly equation

$$G(0,0,0)\equiv\lambda=\frac{e}{4\pi^2f_\pi^3}=9.70\text{ GeV}^{-3} \quad (4)$$

where the zero in the argument of  $G(0,0,0)$  refers to the chiral limit of the massless pions; the number of colors  $N_c$  is equal to 3.

Experimentally,  $\lambda$  is measured at an average photon pion energy of 0.4 GeV and, assuming that there is no momentum dependence in  $G(s,t,u)$ , it is equal to [5]

$$\lambda^{exp}=12.9\pm 0.9\pm 0.5\text{ GeV}^{-3}. \quad (5)$$

The agreement between experiment and theory is not good but certainly corrections will have to be made because measurements made in this experiment are far from the chiral symmetry limit.

The calculations of this process are usually done within vector meson dominance (VMD) models [6–8]. Recently, this process was discussed within the framework of chiral perturbation theory (ChPT) to one loop [9] and also with a combination of ChPT and VMD [10] and the unitarization of the ChPT two-loop amplitude [11].

The purpose of this paper is to investigate the scattering of  $\gamma\pi^0\rightarrow\pi^+\pi^-$  using the dispersion relation, elastic unitarity, and knowledge of the  $P$ -wave pion-pion phase shifts. An integral equation is obtained and is similar to the Muskhelishvili-Omnès (MO) integral equation used in the pion form factor calculation [12]. The integral equation obtained here is, however, much more complicated due to the symmetry of the problem. Its solution can only be obtained by a numerical method.

The pion form factor calculation, using the MO integral equation approach, yields a pion radius too low by 10% and a modulus of the pion form factor at the  $\rho$  resonance also too low by 15%. This is due to the assumption of the elastic unitarity relation which is valid only in the low energy region

below 1.2 GeV but cannot be true at and above the  $\rho'$  (1.5 GeV) region. In order to remove this discrepancy one has to use also, as input, the pion rms radius and hence one has either to make an extra subtraction in the dispersion relation or to make use of the polynomial ambiguity of the solution of the MO equation. One would then get not only the correct value of the absolute value of the pion form factor at the  $\rho$  mass (i.e., the  $\rho$  leptonic width), but also complete agreement with the pion form factor below 1 GeV [4]. The phases of the form factor are of course the experimental  $P$ -wave  $\pi\pi$  phase shifts due to the solution of the MO equation.

We also face the same problem in the calculation of the scattering  $\gamma\pi^0 \rightarrow \pi^+\pi^-$ . The problem could, however, be more serious here than in the pion form factor calculation because of the existence of the  $t$  and  $u$  channels. Not only does the first derivative of the dominant  $P$ -wave amplitude vanish at the energy squared  $s=m_\pi^2$ , but its second derivative at this energy is not accessible to experiments because of the lack of experimental precision.

A further complication is because of the ambiguity of the solution of the integral equation obtained here due to the symmetry of the problem. It is related to but not purely of the polynomial type. For this reason we cannot make a comparable prediction of the  $\gamma\pi^0 \rightarrow \pi^+\pi^-$  cross section at the  $\rho$  mass or the  $\Gamma(\rho \rightarrow \pi\gamma)$  width. The measurement of this width could be used to make a prediction of the energy dependence of  $\gamma\pi^0 \rightarrow \pi^+\pi^-$  away from the  $\rho$  mass and in particular in the low energy region where the the first measurement of  $\lambda$ , Eq. (5), was made.

## II. KINEMATICS AND PARTIAL WAVE PROJECTION

The kinematics of this process are defined as  $s=(k+p_0)^2$ ,  $t=(p_1-p_0)^2$ , and  $u=(p_2-p_0)^2$ . Because all particles involved are on shell, one has  $s+t+u=3m_\pi^2$ . In the center of mass system, in terms of the scattering angle  $\theta$ , we have

$$t = \frac{3m_\pi^2 - s}{2} + \frac{1}{2}(s - m_\pi^2)\sqrt{1 - 4m_\pi^2/s} \cos \theta,$$

$$u = \frac{3m_\pi^2 - s}{2} - \frac{1}{2}(s - m_\pi^2)\sqrt{1 - 4m_\pi^2/s} \cos \theta. \quad (6)$$

The partial wave expansion for  $G(s,t,u)$  is given as follows [11,13]:

$$G(s,t,u) = \sum_{\text{odd } l} G_l(s) P_l'(\cos \theta) \quad (7)$$

where  $\theta$  is the scattering angle and  $P_l'$  is the first derivative of the Legendre polynomial. Hence the lowest partial wave is

$$G_1(s) = \frac{3}{8\pi} \int d\Omega \sin^2 \theta G(s,t,u). \quad (8)$$

In terms of the function  $G_{3\pi}(s,t,u)$  the differential cross section for the process  $\gamma\pi^0 \rightarrow \pi^+\pi^-$  is

$$\frac{d\sigma}{d\cos\theta} = \frac{1}{1024\pi} (s - m_\pi^2) \frac{(s - 4m_\pi^2)^{3/2}}{s^{1/2}} \sin^2 \theta |G(s,t,u)|^2. \quad (9)$$

## III. VECTOR MESON DOMINANCE AND PION FORM FACTOR

Because our integral equation solution is a more sophisticated and precise approach to the vector meson dominance models [14,15], where unitarity and the dispersion relation are extensively used, it cannot avoid the same problems that are present in these models; namely, the solution can be uniquely obtained only when the asymptotic behavior of the solution is specified. It is thus useful to review briefly the VMD models and calculations of the pion form factor with and without introducing the contact term.

### A. Vector meson dominance models for the $\gamma\pi^0 \rightarrow \pi^+\pi^-$ process

Let us consider the VMD models without and with the contact terms for the  $\gamma\pi^0 \rightarrow \pi^+\pi^-$  process as previously discussed in the literature [6,7]. Without the contact term, the VMD model for the  $\gamma\pi^0 \rightarrow \pi^+\pi^-$  amplitude is

$$G^{vmd}(s,t,u) = \frac{\lambda}{3} \left( \frac{m_\rho^2}{m_\rho^2 - s} + \frac{m_\rho^2}{m_\rho^2 - t} + \frac{m_\rho^2}{m_\rho^2 - u} \right) \quad (10)$$

where  $s,t,u$  are the invariant kinematics and  $\lambda$  is defined by Eq. (4). With a contact term, it can be written as

$$G^{vmdc}(s,t,u) = \frac{\lambda}{3-c} \left\{ \frac{m_\rho^2}{m_\rho^2 - s} + \frac{m_\rho^2}{m_\rho^2 - t} + \frac{m_\rho^2}{m_\rho^2 - u} - c \right\} \quad (11)$$

where  $c$  is proportional to the strength of the contact term. Equation (11) can be rearranged to give

$$G^{vmdcc}(s,t,u) = \frac{\lambda}{3} \left\{ \left[ \frac{m_\rho^2}{m_\rho^2 - s} \left( 1 + \frac{c}{3-c} \frac{s}{m_\rho^2} \right) \right] + [s \rightarrow t] + [s \rightarrow u] \right\}. \quad (12)$$

In Eq. (10), the  $\gamma\pi^0 \rightarrow \pi^+\pi^-$  amplitude vanishes as  $s,t,u \rightarrow \infty$  while those in Eqs. (11) and (12) do not vanish because of the presence of the contact term. We have introduced phenomenologically the contact term  $c$  in the scattering  $\gamma\pi^0 \rightarrow \pi^+\pi^-$  without considering how it influences the VMD for the corresponding process  $P \rightarrow \gamma\gamma$ . Assuming complete VMD for  $P \rightarrow \gamma\gamma$ , one has  $c=1$  in order that the Kawarabayashi-Suzuki-Riazuddin-Fayyazuddin (KSRF) relation [17] remains valid [6,7].

The strength of the contact term also influences the value of the second derivative of the  $P$ -wave amplitude at  $s=m_\pi^2$ . Expanding Eq. (11) in a power series of  $s, t, u$ ,

$$G^{vmdc}(s, t, u) = \lambda \left[ 1 + \frac{3}{3-c} \frac{m_\pi^2}{m_\rho^2} + \frac{1}{3-c} \frac{s^2 + t^2 + u^2}{m_\rho^4} + \dots \right], \quad (13)$$

the  $P$ -wave projection of this equation is

$$G_1(s) = \lambda \left[ 1 + \frac{3}{3-c} \frac{m_\pi^2}{m_\rho^2} + \frac{6}{5(3-c)} \frac{(s-m_\pi^2)^2}{m_\rho^4} + \dots \right] \quad (14)$$

where the pion mass is introduced by hand. One has finally

$$\left. \frac{d^2 G_1(s)}{ds^2} \right|_{s=m_\pi^2} = \frac{12}{5(3-c)} \frac{1}{m_\rho^4} \lambda. \quad (15)$$

Instead of characterizing the contact term by the infinite energy behavior of the matrix element, we can specify its presence by evaluating its second derivative for the  $P$  wave at  $s=m_\pi^2$ . For pure VMD,  $c=0$ , it is equal to  $(12/15)\lambda(m_\rho^{-4})$  and for the hidden symmetry model [7],  $c=1$ , it is  $(6/5)\lambda(m_\rho^{-4})$ .

Equation (10) yields a decay width  $\Gamma(\rho\rightarrow\pi\gamma)=36$  keV which is too small compared with the experimental value. Equation (11) for  $c=1$  yields a decay width  $\Gamma(\rho\rightarrow\pi\gamma)=81$  keV in much better agreement with the data (see below). The experimental value of the  $\rho\pi\pi$  coupling or the KSRF relation [17] for the  $\rho\pi\pi$  coupling is used to calculate these widths.

One can improve these equations by making the vector meson  $\rho$  unstable using the self-energy correction for the  $\rho$  propagator [16] and the KSRF relation [17]. This same result can also be obtained using the inverse amplitude for the vector form factor *without* assuming the KSRF relation. The  $\rho$  width obeys the KSRF relation as a consequence of the implementation of the unitarity relation [18]. The factor  $m_\rho^2/(m_\rho^2-s)$  is then replaced by a function  $\Omega(s)$  which is normalized to unity at  $s=0$  and is defined as follows:

$$\Omega(s) = \frac{1}{1 - s/s_R - (1/96\pi^2 f_\pi^2) \{ (s - 4m_\pi^2) H_{\pi\pi}(s) + 2s/3 \}} \quad (16)$$

where  $f_\pi=0.093$  GeV, and  $s_R$  is related to the  $\rho$  mass squared  $m_\rho^2=0.593$  GeV<sup>2</sup> by requiring that the real part of the denominator of Eq. (16) vanish at the  $\rho$  mass;  $H_{\pi\pi}(s)$  is a well-known integral over the phase space factor:

$$H_{\pi\pi}(s) = \begin{cases} 2 - 2 \sqrt{\frac{s-4m_\pi^2}{s}} \ln \frac{\sqrt{s} + \sqrt{s-4m_\pi^2}}{2m_\pi} + i\pi \sqrt{\frac{s-4m_\pi^2}{s}}, & s \geq 4m_\pi^2, \\ 2 - 2 \sqrt{\frac{4m_\pi^2-s}{s}} \arctan \sqrt{\frac{s}{s-4m_\pi^2}}, & 0 \leq s \leq 4m_\pi^2, \\ 2 - 2 \sqrt{\frac{s-4m_\pi^2}{s}} \ln \frac{\sqrt{4m_\pi^2-s} + \sqrt{-s}}{2m_\pi}, & s \leq 0. \end{cases} \quad (17)$$

Let us call the phase of  $\Omega(s)$   $\delta$ . Then  $\Omega(s)$  has the following phase representation:

$$\Omega(s) = \exp \left[ \frac{s}{\pi} \int_{4m_\pi^2}^{\infty} \frac{\delta(z) dz}{z(z-s-i\epsilon)} \right]. \quad (18)$$

The phase  $\delta$  is exactly the elastic  $P$ -wave  $\pi\pi$  phase shift as can be seen from Fig. 1. Alternatively, one can use the experimental phase shift to calculate the function  $\Omega(s)$  but the expression given above is most convenient.

Other functions  $\Omega(s)$  normalized to unity at  $s=s_0$  can be expressed in terms of the function  $\Omega(s)$  by the simple relation  $\Omega(s, s_0) = \Omega(s)/\Omega(s_0)$ .

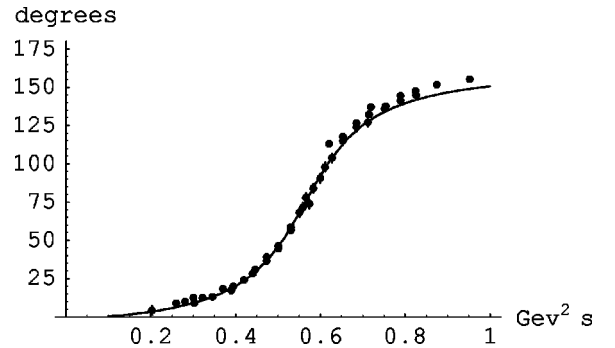


FIG. 1. The phase of the function  $\Omega(s)$  in degrees (vertical axis) is given as a function of  $s$  (GeV<sup>2</sup>). The experimental data are taken from Refs. [27–29].

$\Omega(s)$  as given by Eq. (16) has a ghost pole at  $s = -2.5 \times 10^5 \text{ GeV}^2$  which is far away from the physical region relevant to our calculation and hence is irrelevant for our low energy calculation.

The function  $\Omega(s)$  defined here is the same as the inverse of the  $D$  function given by Ref. [10] except for the definition of the  $\rho$  mass, which is approximate there.

In both approaches, the chiral symmetry limit should be defined as the limit of  $s, t, u$  tending to zero first and then  $m_\pi^2 \rightarrow 0$ . This order should be respected because the branch point at  $s, t, u = 4m_\pi^2$  also goes to zero in the chiral limit. Using this definition we could have calculated  $\bar{\lambda}$  in terms of  $\lambda$  without using the large  $N_c$  limit, but the difference is negligible as discussed previously.

Replacing  $m_\rho^2/(m_\rho^2 - s)$  by  $\Omega(s)$  in Eq. (10) yields  $\Gamma(\rho \rightarrow \pi\gamma) = 42 \text{ keV}$  and with  $c=1$  (the hidden symmetry model with the additional assumption of a complete vector meson dominance model for  $\pi^0 \rightarrow \gamma\gamma$ ) in Eq. (11) this gives  $\Gamma(\rho \rightarrow \pi\gamma) = 95 \text{ keV}$ . The differences between these values and those obtained previously are just due to the  $\rho$  finite width correction. These results show the importance of the presence of the contact term. While the present experimental data for  $\Gamma(\rho \rightarrow \pi\gamma)$  are not settled, it is likely that the result for the hidden symmetry model is favored (see below).

With chiral symmetry broken, the pions acquire a finite but small mass, and Eqs. (10)–(12) become, respectively,

$$G^{vmd}(s, t, u) = \frac{\lambda}{3} \{ \Omega(s) + \Omega(t) + \Omega(u) \}, \quad (19)$$

$$G^{vmdc}(s, t, u) 2 = \frac{\lambda}{3-c} \{ \Omega(s) + \Omega(t) + \Omega(u) - c \}, \quad (20)$$

and

$$G^{vmdcc}(s, t, u) = \frac{\lambda}{3} \left\{ \left[ \Omega(s) \left( 1 + \frac{c}{3-c} \frac{s}{m_\rho^2} \right) \right] + [s \rightarrow t] + [s \rightarrow u] \right\}. \quad (21)$$

Equations (19),(20),(21) do not, however, satisfy the elastic unitarity relation, i.e., the projected  $P$  wave does not have the phase of the  $P$ -wave  $\pi\pi$  interactions below 1 GeV [19] as can be seen in Fig. 3 below. This result is not surprising because the multiple  $\pi\pi$  scattering correction, which should be relevant for this problem, is not taken into account in these equations. The contact term model with  $c=1$  satisfies the phase theorem better than the pure VMD model because of the presence of the contact term significantly increases the magnitude of the resonance term compared with the background terms from the  $t$  and  $u$  channels. This leads us to a smaller correction using the following integral equation approach where the unitarity relation is explicitly built in.

Equations (10),(11),(12) can be considered as the large  $N_c$  limit of QCD. This is true because  $f_\pi^2 \sim N_c$  and the function

$\Omega(s)$  defined by Eq. (16) becomes a simple pole in this limit. We shall elaborate this fact later in this article.

In the following, we shall define the function  $G(s, t, u)$  at the symmetry point  $s = t = u = m_\pi^2$  while the chiral symmetry limit of this function is the chiral anomaly  $\lambda$  given by Eq. (4). How are they related to each other? There is no clean answer to this problem. Chiral perturbation theory could be used. The answer depends, however, on one parameter, the scale parameter [9,11]. We prefer to look at the large  $N_c$  limit to get their relation.

Setting  $s = t = u = 0$  in the chiral limit in Eqs. (10),(11), we have

$$G(s = m_\pi^2, t = m_\pi^2, u = m_\pi^2) \equiv \bar{\lambda} = \lambda \left[ 1 + \frac{3}{3-c} \frac{m_\pi^2}{m_\rho^2} \right]. \quad (22)$$

This expression will be used in the following analysis. For  $c=1$ , we have  $\bar{\lambda} = 1.049\lambda$ , whereas the corresponding value for the one-loop ChPT [9,11], assuming that the scale parameter  $\mu^2 = m_\rho^2$ , is  $\bar{\lambda} = 1.053\lambda$ , which is insignificantly larger. In terms of  $\bar{\lambda}$ , with chiral symmetry broken but in the large  $N_c$  limit, one has

$$G^{vmdc}(s, t, u) = \frac{\bar{\lambda}}{3-c} \left\{ \frac{m_\rho^2 - m_\pi^2}{m_\rho^2 - s} + \frac{m_\rho^2 - m_\pi^2}{m_\rho^2 - t} + \frac{m_\rho^2 - m_\pi^2}{m_\rho^2 - u} - c \right\}. \quad (23)$$

## B. Vector meson model for pion form factor

The solution of the integral for the pion form factor with the assumption of an elastic form factor is

$$V(s) = P_n(s) \Omega(s) \quad (24)$$

where  $\Omega(s)$  is given by Eq. (16),  $P_n(s)$  is a polynomial of degree  $n$  in  $s$  with real coefficients, and  $P_n(0) = 1$ . For a given a set of strong  $P$ -wave  $\pi\pi$  phase shifts, the solution of the MO equation is not unique. One can multiply the solution  $\Omega(s)$  by a real polynomial to get a different set of solutions with different asymptotic conditions. The low energy constraint enables us to fix at least some coefficients of the polynomial.

If one assumes  $P_n(s) = 1$ , the square of the modulus of the pion form factor at the  $\rho$  mass is too small by about 30% (see Fig. 2), and the rms radius of the pion is too small by 10%. Constraining the rms radius to be equal to its experimental value, we have to set [20]  $P_n(s) = 1 + 0.15(s/m_\rho^2)$  or

$$V(s) = \left( 1 + 0.15 \frac{s}{m_\rho^2} \right) \Omega(s). \quad (25)$$

The connection between this equation and the contact term was recently discussed [21]. The following integral equation for the process  $\gamma\pi \rightarrow \pi\pi$  is more complicated because the integral equation involves both right and left cuts on the real axis and hence the ambiguity of the solution is not simply the



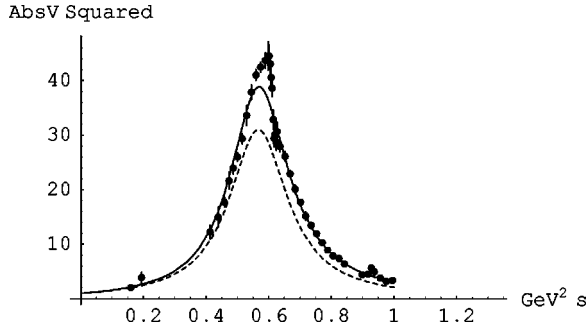


FIG. 2. The square of the modulus of the function  $\Omega(s)$  (vertical axis) is given as a function of  $s$  in  $\text{GeV}^2$  (dashed line). The square of the modulus of the pion form factor  $V(s)$  from Eq. (25) is also shown (solid line). Experimental data are taken from Refs. [30,31].

polynomial ambiguity but is only related to it. It can be obtained only by solving the integral equation numerically as will be shown below.

#### IV. INTEGRAL EQUATION APPROACH USING ELASTIC UNITARITY RELATION

In this article, the process  $\gamma\pi\rightarrow\pi\pi$  is studied using the dispersion relation and elastic unitarity for the lowest partial wave. An integral equation of the type of the Muskhelishvili-Omnès integral equation [12] is obtained. The difference is that the integral equation to be treated here is much more complicated because of crossing symmetry; no exact solution has been found. We shall get the solution of this integral equation by an iterative procedure, but with the crucial property that the iterative solution for the lowest partial wave satisfies the phase theorem at every step as required by unitarity [19]. As the solution of the MO equation is ambiguous by a polynomial, we find a similar problem here. But the ambiguity is not the same, i.e., a new solution cannot be obtained by multiplying the old solution by a polynomial.

We start first by deriving the dispersion relation of the single variables  $s, t, u$  for  $\gamma\pi\rightarrow\pi\pi$ ; we then project out the  $P$ -wave amplitude where the rescattering effect is important because of the presence of the low energy  $\rho$  resonance at 0.77 GeV. The rescattering effect is supposed to be negligible for higher partial waves because there are no resonances below 1.5 GeV for the two pions in  $F, H$ , etc., waves. After solving the integral equation numerically, one should put the results obtained into the form of the single variable dispersion relation. The crucial point is that the single variable dispersion relation for the scattering amplitude does not satisfy the phase theorem, but its  $P$ -wave projection does.

The integral equation can be derived using the technique of Roy's equation for  $\pi\pi\rightarrow\pi\pi$  scattering [22]. We begin by writing a twice subtracted dispersion relation for  $G(s, t, u)$  at a fixed  $t$ . This dispersion relation can be shown to be valid in general. Using the same technique as that used in obtaining the Roy's equation, namely, using the fixed  $t$  dispersion relation, crossing symmetry, and keeping only the  $P$  wave for the partial wave expansion of the absorptive part, one arrives at

$$G(s, t, u) = \bar{\lambda} + \left[ \frac{(s - m_\pi^2)^2}{\pi} \int_{4m_\pi^2}^{\infty} \frac{\sigma(z) dz}{(z - m_\pi^2)^2 (z - s - i\epsilon)} \right] + [s \leftrightarrow t] + [s \leftrightarrow u] \quad (26)$$

(for an explicit demonstration of this equation, see Ref. [11]), where the symmetry point in the problem is at  $s = t = u = m_\pi^2$ , and  $\bar{\lambda}$ , is related to  $\lambda$ , as will be discussed later. The subtracted linear terms do not contribute because they are proportional to  $(s - m_\pi^2) + (t - m_\pi^2) + (u - m_\pi^2) = 0$ . One can make a partial fraction of the dispersion integral to show that one can equally well work with the once subtracted dispersion relation, which we shall use in the following:

$$G(s, t, u) = \bar{\lambda} + \left[ \frac{(s - m_\pi^2)}{\pi} \int_{4m_\pi^2}^{\infty} \frac{\text{Im } G_1(z) dz}{(z - m_\pi^2)(z - s - i\epsilon)} \right] + [s \leftrightarrow t] + [s \leftrightarrow u] = A(s) + A(t) + A(u), \quad (27)$$

where  $\text{Im } G_1(z)$  is the imaginary part of the  $P$ -wave amplitude.

The assumption of the dominance of the  $P$ -wave amplitude made to get the integral equation can be experimentally checked by measuring the absence of deviation from the  $\sin^2 \theta$  angular distribution given by Eq. (9). Should this assumption be incorrect, one could try to treat the contribution of the higher partial waves in the  $\rho$  region phenomenologically by using some real amplitudes [11].

Let us denote by  $G_1(s)$  the lowest  $P$  partial wave projection of  $G(s, t, u)$  as given by Eq. (8). The elastic unitarity relation gives

$$\text{Im } G_1(s) = G_1(s) e^{-i\delta(s)} \sin \delta(s) \quad (28)$$

where  $\delta$  is the  $P$ -wave  $\pi\pi$  phase shift obtained from the available experimental data, which show that it passes through  $90^\circ$  at the  $\rho$  mass as can be seen from Fig. 1. There is no measurable inelastic effect below 1.2 GeV. Projecting out the  $P$  wave from Eq. (27) and interchanging the order of integration, we have

$$G_1(s) = \bar{\lambda} + \frac{s - m_\pi^2}{\pi} \int_{4m_\pi^2}^{\infty} \frac{G_1(z) e^{-i\delta(z)} \sin \delta(z)}{(z - m_\pi^2)(z - s - i\epsilon)} dz + \frac{3}{2\pi} \int_{4m_\pi^2}^{\infty} G_1(z) e^{-i\delta(z)} \sin \delta(z) \times \left\{ \frac{1}{b(s)} \left( 1 - \frac{[z - a(s)]^2}{b(s)^2} \right) \ln \left| \frac{z - a(s) + b(s)}{z - a(s) - b(s)} \right| + 2 \frac{z - a(s)}{b(s)^2} - \frac{4}{3(z - m_\pi^2)} \right\} dz. \quad (29)$$

The first derivative of  $G_1(s)$  at  $s = m_\pi^2$  vanishes and its second derivative with respect to  $s$  evaluated at  $s = m_\pi^2$  is

$$\left. \frac{d^2 G_1(s)}{ds^2} \right|_{s=m_\pi^2} = \frac{12}{5\pi} \int_{4m_\pi^2}^{\infty} \frac{\text{Im} G_1(z) dz}{(z-m_\pi^2)^3}. \quad (30)$$

The standard solution of the MO equation is ambiguous by a polynomial, but the problem here is much more complicated because of the symmetry of the  $s, t, u$  channels, which leads to a much more complicated integral equation, and hence it does not have the same type of ambiguity. Equation (29) is a complicated integral equation. It is similar to, but more complicated than, the Muskelishvili-Omnes type [12], because the  $t$  and  $u$  channel contributions are also expressed in terms of the unknown function  $G_1(s)$ . It should be noticed that the first term has a cut from  $4m_\pi^2$  to  $\infty$  and the second one has a cut from 0 to  $-\infty$ . For  $s \geq 4m_\pi^2$  the argument of the logarithm function in Eq. (29) never vanishes and hence this enables one to solve the integral equation by the following iteration scheme which converges very fast.

### Iterative solutions

As remarked above, the integral equation (29) has both right and left cuts. In setting up the iterative scheme, it is important to keep in mind that the final solution should be symmetric in the  $s, t, u$  variables as given by Eq. (27). Because of this analytical structure, we can define an iteration procedure that consists of splitting Eq. (29) into two separate equations:

$$G_1^{(i)}(s) = \frac{\bar{\lambda}}{3} + T_B^{(i-1)}(s) + \frac{s-m_\pi^2}{\pi} \times \int_{4m_\pi^2}^{\infty} \frac{G_1^{(i)}(z) e^{-i\delta(z)} \sin \delta(z)}{(z-m_\pi^2)(z-s-i\epsilon)} dz \quad (31)$$

and

$$T_B^{(i-1)}(s) = \frac{2\bar{\lambda}}{3} + \frac{3}{2\pi} \int_{4m_\pi^2}^{\infty} G_1^{(i)}(z) e^{-i\delta(z)} \sin \delta(z) \times \left\{ \frac{1}{b(s)} \left( 1 - \frac{[z-a(s)]^2}{b(s)^2} \right) \ln \left| \frac{z-a(s)+b(s)}{z-a(s)-b(s)} \right| + 2 \frac{z-a(s)}{b(s)^2} - \frac{4}{3(z-m_\pi^2)} \right\} dz, \quad (32)$$

where  $i \geq 1$  and  $G_1^{(i)}$  is the value of the function  $G_1(s)$  calculated at the  $i$ th step in the iteration procedure; the Born term  $T_B^{i-1}(s)$  is calculated at the  $(i-1)$ th step. An iteration cycle is defined as a numerical calculation of both these equations.

The Born term is real for  $s \geq 0$  and has a left cut in  $s$  for  $s < 0$ . In writing Eqs. (31),(32), care was taken to preserve the symmetry in the  $s, t, u$  variables for the function  $F(s, t, u)$ , which requires us to split the subtraction constant  $\bar{\lambda}$  in Eq. (29) symmetrically into three equal pieces; one piece contributes to Eq. (31) and the other two to Eq. (32).

The solution of the integral equation Eq. (31) is of the MO type [12]:

$$G_1^{(i)}(s) = \frac{\bar{\lambda}}{3} \bar{\Omega}(s, m_\pi^2) + T_B^{(i-1)}(s) + \bar{\Omega}(s, m_\pi^2) \frac{s-m_\pi^2}{\pi} \times \int_{4m_\pi^2}^{\infty} \frac{\bar{\Omega}^{-1}(z, m_\pi^2) e^{i\delta(z)} \sin \delta(z) T_B^{(i-1)}(z) dz}{(z-m_\pi^2)(z-s-i\epsilon)} \quad (33)$$

where

$$\bar{\Omega}(s, m_\pi^2) = \frac{P_n(s) \Omega(s)}{P_n(m_\pi^2) \Omega(m_\pi^2)}, \quad (34)$$

i.e., this new function  $\bar{\Omega}$  is normalized to unity at  $s = m_\pi^2$  and  $P_n(s)$  is a polynomial of the  $n$ th degree with real coefficients. In the following, as in Eq. (25), we take only the first two terms in the polynomial and hence set

$$P_n(s) = 1 + \alpha \frac{s}{m_\rho^2}, \quad (35)$$

where  $\alpha$  is a parameter that is related to the contact term  $c$  defined previously. The second derivative of the  $P$ -wave amplitude, defined by the sum rule Eq. (30), depends sensitively on the parameter  $\alpha$ .

Equation (33) is not really a typical solution written down for this type of integral equation. It is usually written in terms of the ‘‘driving’’ term  $T_B^{(i-1)}(z)$ . This procedure is not at all valid for the present situation; we must modify it in order to get a final solution for the full amplitude that is completely symmetric in the  $s, t, u$  variables. Equation (33) is written with this fact in mind. The first term on its right-hand side (RHS) represents the VMD in the  $s$  channel with or without a contact term, the second term is the corresponding contribution from the  $t$  and  $u$  channels, and the third term is the rescattering due to the final state interaction in the  $s$  channel.

At first sight one would think that the RHS of Eq. (33) does not have the  $P$ -wave phase  $\delta$ . This is not so, because we first note that the last integral can be separated into a principal part integral and a delta-function contribution which is purely imaginary. Then combining this delta-function contribution with  $T_B^{(i-1)}(s)$  in Eq. (33), we have

$$G_1^{(i)}(s) = \bar{\Omega}(s, m_\pi^2) \left\{ \frac{\bar{\lambda}}{3} + T_B^{(i-1)}(s) \text{Re}[\bar{\Omega}^{-1}(s, m_\pi^2)] + \frac{s-m_\pi^2}{\pi} \times \text{P} \int_{4m_\pi^2}^{\infty} \frac{\bar{\Omega}^{-1}(z, m_\pi^2) e^{i\delta(z)} \sin \delta(z) T_B^{(i-1)}(z) dz}{(z-m_\pi^2)(z-s)} \right\}, \quad (36)$$

where P stands for the principal part integration. We have made the usual decomposition  $N/D$  for the partial wave amplitude, which can be shown to be quite general and inde-

pendent of any dynamical scheme:  $e^{i\delta}\sin\delta(s) = N(s)\rho(s)\bar{\Omega}(s,m_\pi^2)$  where  $N(s)$  contains only the left-hand cut,  $D^{-1}(s) = \bar{\Omega}(s)$  contains only the right-hand cut, and  $\rho(s) = \sqrt{(1-4m_\pi^2/s)}$ . Equation (36) shows that indeed  $G_1^{(i)}(s)$  has the phase  $\delta$ .

One arbitrarily defines the convergence of the iteration scheme at the  $i$ th iteration step when  $|G_1^{(i)}|/|G_1^{(i-1)}|$  differs from 1 by less than 1% or so in the energy range from the two-pion threshold to 1 GeV. (Alternatively, one can also require that the ratio  $|T_B^{(i)}|/|T_B^{(i-1)}|$  be unity within an accuracy of 1%.)

Once the solution for the partial wave is obtained, one should return to the calculation of the full amplitude. This can be done by combining the  $T_B^{(i-1)}$  Born term in Eq. (33) with higher uncorrected partial waves (for rescattering) from the  $t$  and  $u$  channels to get the final solution:

$$G^{(i)}(s,t,u) = \frac{\bar{\lambda}}{3} \left( \{\bar{\Omega}(s,m_\pi^2)[1+3I^{(i-1)}(s)]\} + \{(s\leftrightarrow t)\} + \{(s\leftrightarrow u)\} \right), \quad (37)$$

where the function  $I^{(i-1)}$  denotes the multiple rescattering correction:

$$I^{(i-1)}(s) = \frac{s-m_\pi^2}{\pi} \int_{4m_\pi^2}^{\infty} \frac{\bar{\Omega}^{-1}(z,m_\pi^2) e^{i\delta(z)} \sin\delta(z) T_B^{i-1}(z) dz}{(z-m_\pi^2)(z-s-i\epsilon)}. \quad (38)$$

It is obvious that  $G^{(i)}(s,t,u)$  does not have the phase  $\delta$  of the  $P$ -wave  $\pi\pi$  scattering, but its  $P$ -wave projection does. This is so because, projecting out the  $l=1$  partial wave from Eq. (37), we arrive at Eq. (33) with  $T_B^{i-1}(s)$  replaced by  $T_B^i(s)$ . Because of the assumed criterion for the convergence of the iteration scheme,  $T_B^{i-1}(s) \simeq T_B^i(s)$ , it is easily seen that  $G_1^{(i)}(s)$  has the phase  $\delta$ , using the results of Eq. (33) and Eq. (36). The remaining higher partial waves  $l>1$  are all real because we have assumed that the strong final state interactions of the higher partial waves are negligible. The final solution Eq. (37) is completely symmetric in the  $s,t,u$  variables.

## V. NUMERICAL SOLUTIONS

We shall solve our integral equation numerically for various values of  $\alpha$  defined by Eq. (35), corresponding to different values of the contact terms as discussed in Eq. (11). We examine the following cases:  $\alpha=0,0.30,0.50,0.70$ . The iteration scheme can be done by first guessing a solution for  $T_B(s)$  corresponding to a chosen value of  $\alpha$ . We can take a rather arbitrary first solution for this function. For example, for a given  $\alpha$  we can take the  $t$  and  $u$  channel contribution to the Born term as

$$T_B^0(s) = \frac{3}{4} \int_{-1}^1 d\cos\theta \sin^2\theta \frac{\bar{\lambda}}{3} \left\{ \left[ \frac{m_\rho^2 - m_\pi^2}{m_\rho^2 - t} \right] + \left[ \frac{m_\rho^2 - m_\pi^2}{m_\rho^2 - u} \right] \right\}, \quad (39)$$

which is independent of  $\alpha$ . With this expression for the Born term, the iteration scheme can be started by calculating the solution of the integral equation as given by Eq. (33). The next step is to calculate the Born term by Eq. (32); there is no arbitrariness at this step. The iteration scheme is continued until convergence of the solution is obtained.

The number of iterations depends on the original choice of the Born term i.e., how close it is to the final solution. Even for a not very good approximation for  $T_B^{(0)}$  such as that given by Eq. (39), it is found that after one iteration one can already reach a reasonable approximation for the solution of the integral equation.

Convergence to the final solution for  $\alpha=0.3,0.5,0.7$ , with a precision of the order of 1% or better, could be achieved without using the iteration scheme if one chose a good expression for  $T_B^0(s)$ . For this purpose, one can use instead the Born terms calculated from the following zero width contribution of the  $t$  and  $u$  channels of Eq. (11), which depends on the strength of the contact term:

$$T_B^0(s) = \frac{3}{4} \int_{-1}^1 d\cos\theta \sin^2\theta \frac{\bar{\lambda}(1+\alpha)}{3} \times \left\{ \left[ \frac{m_\rho^2 - m_\pi^2}{m_\rho^2 - t} \right] + \left[ \frac{m_\rho^2 - m_\pi^2}{m_\rho^2 - u} \right] - \frac{2\alpha}{1+\alpha} \right\} \quad (40)$$

where we have used the large  $N_c$  relation

$$\alpha = \frac{c}{3-c}. \quad (41)$$

We make use of this relation here to calculate the Born terms and also to get the relation between  $\lambda$  and  $\bar{\lambda}$ .

Equation (40) is obtained in the limit of a narrow  $\rho$  width. As discussed above, this limit is obtained when we let the number of colors  $N_c \rightarrow \infty$ . In this limit, as will be shown below, Eq. (37) becomes Eq. (11) or Eq. (12). The pure VMD model corresponds to  $\alpha=0$  and for models with the contact term  $c=1$ , e.g., the hidden symmetry model [7],  $\alpha=1/2$ . (More precisely, the hidden symmetry model with no contact term in the pseudoscalar mesons decaying into two gammas requires  $c=1$ .) For the real situation where  $N_c=3$  there should be a substantial correction to this relation.

For  $\alpha=0$ , without an iteration of the integral equation, one can get a precision only of the order of 5%. For other values of  $\alpha$ , using Eq. (40) for the Born terms, and without going through the iteration scheme, one can already achieve a precision of better than 1% using only Eq. (31). For  $\alpha=0$ , after five iterations a precision of better than 1% is reached. For other values of  $\alpha=0.3,0.5,0.7$  a precision of better than  $10^{-3}\%$  is reached after only four iterations. These numbers indicate that the rescattering effect is much more important for  $\alpha=0$  and much less important for other values of  $\alpha$ .

The slow convergence of the iteration scheme for  $\alpha=0$  is due to a large violation of the phase theorem at the zeroth

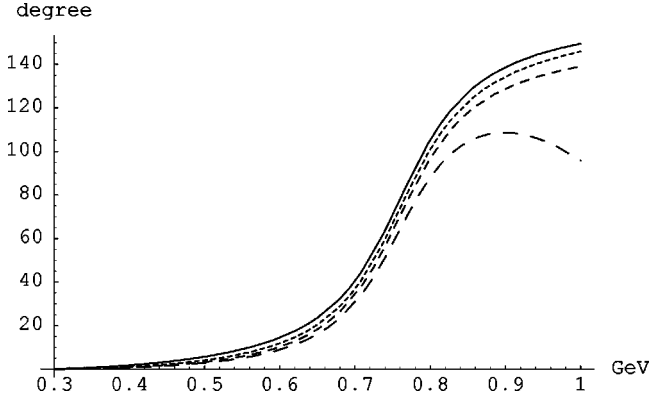


FIG. 3. The  $P$ -wave strong  $\pi\pi$  phase shift (vertical axis) as a function of the energy is shown by the solid line. The projected  $P$ -wave amplitude phase of  $\gamma\pi^0 \rightarrow \pi^+\pi^-$  as given by the VMD model without contact term, Eq. (19), is given by the long dashed line; with the contact term  $c=1$ , Eq. (20), by the short dashed line; with the contact term  $c=1$ , Eq. (21), by the medium dashed line.

order as shown in Fig. 3. For other cases the violation of the phase theorem is not so serious and even without the iteration scheme one can already get an approximate solution accurate to better than 1% by directly solving the integral equation as discussed above.

Instead of parametrizing our solution by the value of  $\alpha$ , it is more physical to describe the solution as a function of the width  $\Gamma(\rho \rightarrow \pi\gamma)$ . This quantity is not unambiguous and will be defined in the following section. It is denoted by  $\Gamma(\rho \rightarrow \pi\gamma)$  using our definition while the corresponding partial width using the usual Breit-Wigner parametrization is denoted by  $\Gamma(\rho \rightarrow \pi\gamma)_{bw}$  with the value of the  $\rho$  mass the same as in our definition, i.e.,  $m_\rho^2 = 0.593 \text{ GeV}^2$  and  $\Gamma(\rho \rightarrow \pi\pi) = 0.156 \text{ GeV}$ . There is a substantial difference for the values of  $\Gamma(\rho \rightarrow \pi\gamma)$  using these two definitions. In Table I  $\Gamma(\rho \rightarrow \pi\gamma)$ ,  $\Gamma(\rho \rightarrow \pi\gamma)_{bw}$ , and the second derivative of the  $P$ -wave amplitude at  $s = m_\pi^2$  are given as functions of the numerical value of  $\alpha$ .

For various values of  $\alpha$ , the square of the absolute value of the  $P$ -wave amplitude  $G_1(s)$ , in units of  $\bar{\lambda}^2$ , is plotted against the energy squared  $s$ , in Fig. 4 and Fig. 5. It is seen

TABLE I. Solution of the  $P$ -wave amplitude for the  $\gamma\pi \rightarrow \pi\pi$  integral equation as a function of the parameter  $\alpha$ . The second column is  $\Gamma(\rho \rightarrow \pi\gamma)$  in keV according to the definition given in the text. The third column is  $\Gamma(\rho \rightarrow \pi\gamma)_{bw}$  in keV using the Breit-Wigner formula Eq. (45) evaluated at the maximum of the cross section. The fourth column is the second derivatives of the  $P$ -wave amplitude at the point  $s = m_\pi^2$  in  $\text{GeV}^{-2}$ .

| $\alpha$ | $\Gamma(\rho \rightarrow \pi\gamma)$<br>(keV) | $\Gamma(\rho \rightarrow \pi\gamma)_{bw}$<br>(keV) | $\bar{\lambda}^{-1} d^2 G_1(s) / ds^2 (s = m_\pi^2)$<br>$\text{GeV}^{-2}$ |
|----------|-----------------------------------------------|----------------------------------------------------|---------------------------------------------------------------------------|
| 0.00     | 50.7                                          | 57.8                                               | 4.88                                                                      |
| 0.30     | 68.0                                          | 76.4                                               | 5.30                                                                      |
| 0.50     | 84.3                                          | 91.8                                               | 5.64                                                                      |
| 0.70     | 103                                           | 111                                                | 6.00                                                                      |

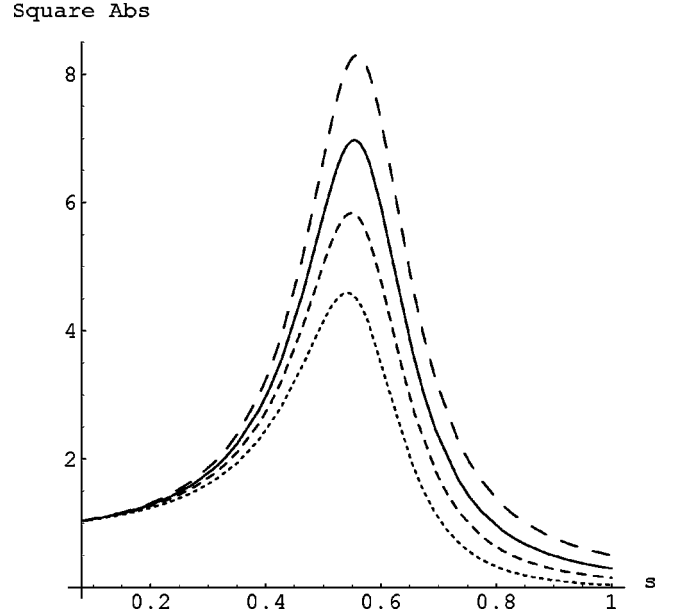


FIG. 4. Plot of the square of the absolute value of the  $P$ -wave amplitude  $|G_1(s)|^2$  in units of  $\bar{\lambda}^2$  as a function of  $s$  in  $\text{GeV}^2$  for  $\alpha=0.5$  (solid line);  $\alpha=0.0$  (short dashed line);  $\alpha=0.3$  (medium dashed line);  $\alpha=0.7$  (long dashed line).

that the larger the values of  $\alpha$  the higher are the maximum values of the  $P$ -wave amplitude.

In Fig. 6 the modulus of the ratio  $3G_1(s)/\bar{\Omega}(s)$  is plotted against the energy squared  $s$  ( $\text{GeV}^2$ ); this ratio indicates the deviation from the Breit-Wigner form as given by the function  $\bar{\Omega}(s)$ .

For various values of  $\alpha$ , accurate values (to better than 1%) of the modulus of the  $P$ -wave amplitude from the two-

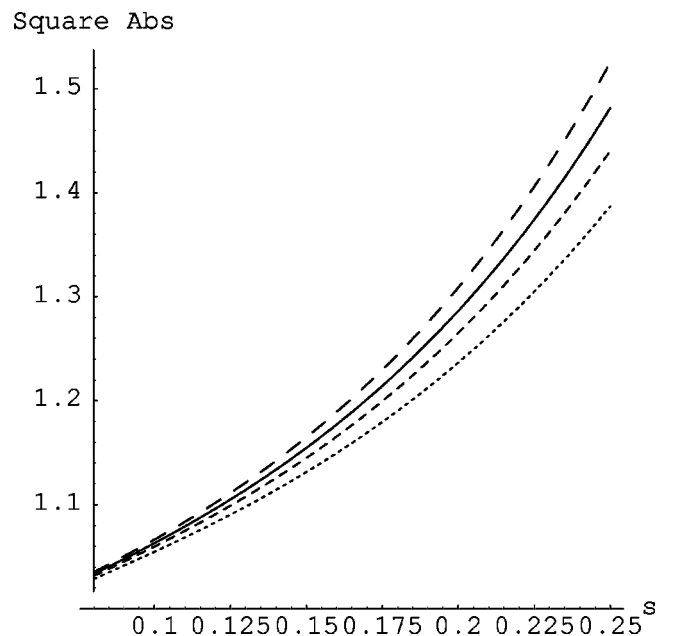


FIG. 5. Same as Fig. 4 but with  $0.08 \text{ GeV}^2 \leq s \leq 0.25 \text{ GeV}^2$ .



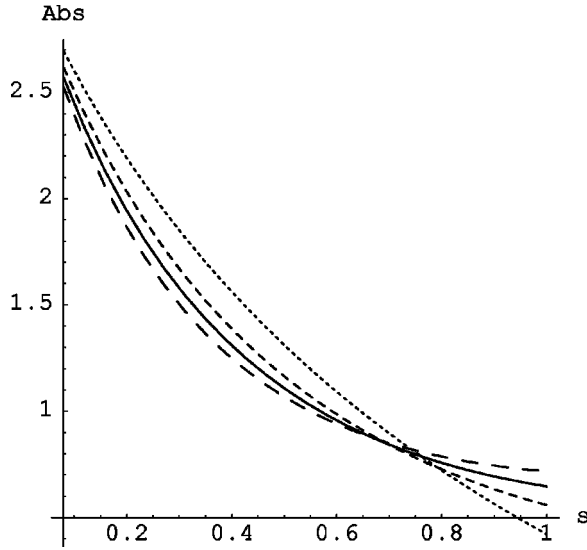


FIG. 6. Plot of the ratio  $|3G_1(s)/\Omega(s, m_\pi^2)|$  in units of  $\bar{\lambda}$  for various values of  $\alpha$ . The curves are the same as in Fig. 4.

pion threshold to 1 GeV can be obtained by using the modulus of  $\bar{\Omega}(s)$  divided the function  $C(s)$  given in Table II:

$$G_1(s) = \bar{\Omega}(s, m_\pi^2) C(s) \frac{\bar{\lambda}}{3}. \quad (42)$$

We are also interested in finding the corrections due to the multiscattering effect in the VMD approximation to the function  $A(s)$  defined by Eq. (27) and given by Eq. (37):

$$A(s) = \bar{\Omega}(s, m_\pi^2) J(s) \quad (43)$$

or

$$J(s) = \frac{\bar{\lambda}}{3} [1 + 3I^{i-1}(s)] \quad (44)$$

for the value of  $i$  attained at the end of the iteration of the integral equation. In Fig. 7 the modulus of  $J(s)$  is plotted against the energy squared  $s$  in units of  $\text{GeV}^2$ . If there were no corrections to the VMD model,  $J(s)$  would be unity. It is seen that the corrections are most important for the case of  $\alpha=0$ .

In Fig. 8 the phase of  $A(s)$  is also plotted against the energy squared  $s$  for various values of  $\alpha$  and compared with the  $P$ -wave  $\pi\pi$  phase shift.

TABLE II. Relation between the  $P$ -wave amplitude  $G_1(s)$  and  $\bar{\Omega}(s, m_\pi^2)$  as given by the function  $C(s)$  defined by Eq. (42) in the text.

| $\alpha$ | $1/C(s)$                                 |
|----------|------------------------------------------|
| 0.00     | $2.457s^3 - 1.662s^2 + 1.162s + 0.2813$  |
| 0.30     | $0.808s^2 + 0.667s + 0.3250$             |
| 0.50     | $-0.759s^3 + 1.278s^2 + 0.705s + 0.3267$ |
| 0.70     | $-1.015s^3 + 1.183s^2 + 0.898s + 0.318$  |

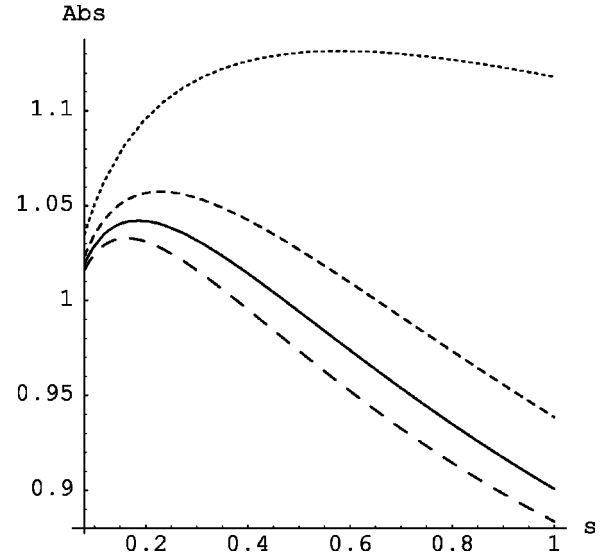


FIG. 7. Plot of the absolute value of the function  $J(s)$  defined by Eq. (43) in units of  $\bar{\lambda}$  as a function of  $s$  in  $\text{GeV}^2$ . The curves are the same as in Fig. 4.

In Fig. 9,  $|G(s, t, u)|^2$  with  $\cos\theta=0$  and  $\cos\theta=0.75$  are plotted against  $s$  (in  $\text{GeV}^2$ ) for the special case  $\alpha=0.5$ . Figures with other values of  $\alpha$  and  $\cos\theta$  are not shown because they are quite similar to Fig. 9. Therefore the higher partial waves are completely negligible for energies below 1 GeV.

## VI. COMPARISON WITH EXPERIMENTAL DATA AND OTHER THEORETICAL WORK

Our calculation can be compared with experimental data at low and high energy. At low energy, the only experimental data available are given by Ref. [5]. From Fig. 5, at an en-

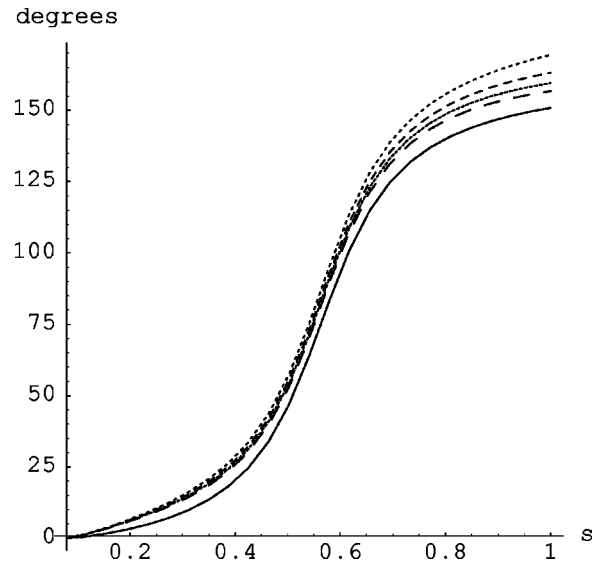


FIG. 8. Plot of the phase of the function  $A(s)$  defined by Eq. (43) as a function of  $s$  in  $\text{GeV}^2$ . The solid line represents the  $P$ -wave strong  $\pi\pi$  phase shift; the dotted line,  $\alpha=0.5$ ; the short dashed line,  $\alpha=0.0$ ; the medium dashed line,  $\alpha=0.3$ , the long dashed line,  $\alpha=0.7$ .

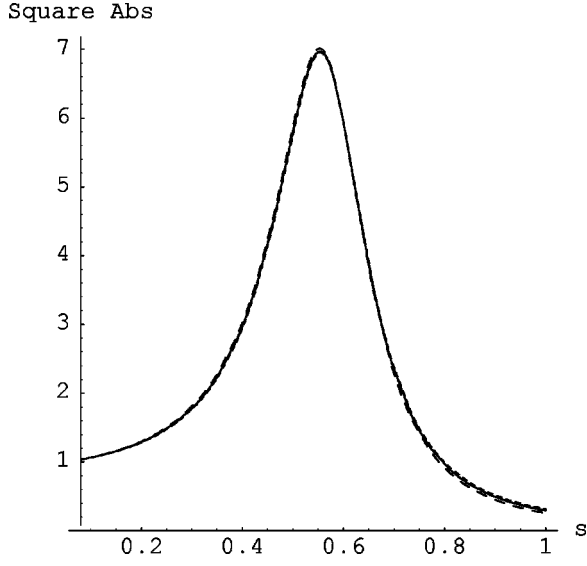


FIG. 9. Square of the modulus of  $G(s, t, u)$  in units of  $\bar{\lambda}^2$  with  $\cos \theta = 0$  (long dashed line), and  $\cos \theta = 0.7$  (short dashed line), and the square of the modulus of the  $P$ -wave amplitude  $G_1(s)$  (solid line) for  $\alpha = 0.5$  as functions of  $s$  in  $\text{GeV}^2$ .

ergy  $s \approx 0.16 \text{ GeV}^2$ , corresponding to the average energy measured in Ref. [5] we have, for  $\alpha = 0.5$ ,  $|G_1(s)| \approx |G(s, t = u)| = 1.15\lambda$ , which is about one standard deviation smaller than the measured value  $(1.29 \pm 0.09 \pm 0.05)\lambda$ . It is clearly important to improve the precision of this experiment.

At higher energy, the experimental cross section for  $\gamma\pi \rightarrow \pi\pi$  is usually analyzed in terms of the Breit-Wigner formula:

$$\frac{d\sigma}{ds} = \frac{24\pi s}{(s - m_\pi^2)^2} \frac{m_\rho^2 \Gamma(\rho \rightarrow 2\pi) \Gamma(\rho \rightarrow \pi\gamma)}{(m_\rho^2 - s)^2 + m_\rho^2 \Gamma_\rho^2(s)}. \quad (45)$$

This formula is usually not accurate because it either neglects the contribution of the part of the amplitude from the  $t$  and  $u$  channels or assumes that the cross section can be fitted with a Breit-Wigner form, which may not be true. Furthermore, the maximum of the modulus of the  $P$ -wave amplitude is shifted significantly toward lower energy, which complicates analysis of the experimental data using Eq. (45).

The result of our calculation shows that, at the maximum of the absolute value of the  $P$ -wave amplitude, the phase of the amplitude is not  $90^\circ$ . The only method that we find acceptable is to define the  $\rho$  mass as the value of  $s$  when the phase of the function  $\Omega$ , which is the same as the experimental  $P$ -wave  $\pi\pi$  phase shift, passes through  $90^\circ$ . Its width is proportional to the inverse of the derivative with respect to  $s$  of  $\cot \delta$  at  $s = m_\rho^2$ :

$$\frac{1}{m_\rho \Gamma_\rho} = \frac{d}{ds} \cot \delta(s) \Big|_{s=m_\rho^2}. \quad (46)$$

With this definition the  $\rho$  width as given by Eq. (16) is 0.156 GeV. One can then use the  $P$ -wave cross section at  $s = m_\rho^2$  to calculate the width  $\Gamma(\rho \rightarrow \pi\gamma)$  using Eq. (45). The value

obtained is denoted by  $\Gamma(\rho \rightarrow \pi\gamma)$  and is approximately 10% lower than the value obtained by using the maximum observed  $\gamma\pi \rightarrow \pi\pi$  cross section in combination with the Breit-Wigner formula, Eq. (45), which is now denoted by  $\Gamma(\rho \rightarrow \pi\gamma)_{bw}$  (see Table I).

Using our method, we could even integrate the measured cross section on either side of the  $\rho$  mass by 0.1 GeV in order to improve the experimental accuracy without changing its value by more than 1%. This precision would not be possible if one did the calculation with the  $\rho$  mass as the value of the maximum cross section.

The present experimental results are not consistent with each other. The more recently published experimental results by Caparo *et al.* gave the value for  $\Gamma(\rho \rightarrow \pi\gamma) = 81 \pm 4 \pm 4 \text{ keV}$  [23], whereas earlier results by Huston *et al.* gave a lower value [24]. These two experiments were Primakoff-like experiments using a high energy charged pion beam on a heavy target. The experimental result from  $e^+e^-$  reaction gives a higher value for the  $\rho \rightarrow \pi\gamma$  width [26] but has a large error.

A more recent unpublished result using photoproduction of a pair of pions off a nucleon target yields  $\Gamma(\rho \rightarrow \pi\gamma)_{bw} = 96 \pm 12 \text{ keV}$  [25]. Unlike the two previous Primakoff experiments, this experiment might have some difficulties in isolating the data corresponding to the one-pion exchange diagram from the background effect; one must also take into account the fact that the exchanged pion is off its mass shell.

Because of the lack of experimental information on the second derivative of the  $P$ -wave amplitude at  $s = 0$  or the parameter  $\alpha$  (see Table I), we cannot predict the solution of the integral equation to get the  $\Gamma(\rho \rightarrow \pi\gamma)$  width.

Corresponding to a naive pure VMD model without a contact term, from Table I, our calculation with  $\alpha = 0$  yields a width of  $\Gamma(\rho \rightarrow \pi\gamma) = 50.7 \text{ keV}$  or  $\Gamma(\rho \rightarrow \pi\gamma)_{bw} = 57.8 \text{ keV}$ , whereas, corresponding to the hidden symmetry model with  $c = 1$ , our calculation with  $\alpha = 0.5$  yields  $\Gamma(\rho \rightarrow \pi\gamma) = 84.3 \text{ keV}$  or  $\Gamma(\rho \rightarrow \pi\gamma)_{bw} = 91.8 \text{ keV}$ . With  $\alpha = 0.5$  the value for  $\Gamma(\rho \rightarrow \pi\gamma)_{bw}$  is somewhat smaller than the value of 96 keV obtained by Hannah using the Padé or inverse amplitude method for the ChPT two-loop amplitude, which was calculated numerically [11]. For this special value of  $\alpha$ , one would also recover the main result of the hidden symmetry model with  $c = 1$ . The low energy parameters  $\bar{C}$  and  $\bar{D}$ , corresponding to the first and second derivatives of the function  $A(s)$ , Eq. (43), defined and evaluated by Hannah [11] are in agreement to an accuracy of 2% with those from our integral equation approach. The difference between this work and that of Hannah is presumably due to the interpretation of Eq. (45), the treatment of the multiple scattering effects, and also the interpretation of the contact term. Hannah's work shows the importance of resummation of the perturbation series by the inverse amplitude or Padé method.

There is a similar treatment of this problem by Holstein [10]. The Holstein solution was obtained by taking the product of three functions:

$$G_1^H(s, t, u) = \lambda P_n(s, t, u) \Omega(s) \Omega(t) \Omega(u) \quad (47)$$

where  $P_n(s, t, u)$  is a polynomial in  $s, t, u$  constructed in such

a way that this equation has the same low energy limit as that given by ChPT. The merit of this equation is that the phase theorem is explicitly obeyed as can be seen by projecting out the  $P$  wave from this equation. But this equation is not right because all higher partial waves such as  $F$ ,  $H$ , etc., have the  $\rho$  resonance or they all have the phase of the  $P$ -wave phase shift which is not correct. The singularity associated with the multiple scattering effects that are present in our integral equation approach is not contained in Eq. (47). All possible solutions that can be written in terms of the product of three functions in  $s, t, u$  variables will have this problem. An exception is the problem involving three hadrons with two light particles having no interactions between them, but they interact with an infinitely heavy target.

Holstein's solution yields a comparable value for  $\Gamma(\rho\rightarrow\pi\gamma)_{bw}$  as does our solution with  $\alpha=0.5$ . This result is not surprising because the value of the second derivative of his solution at  $s=m_\pi^2$  is also comparable with ours. His solution can be fixed by projecting out the  $P$ -wave imaginary part and putting it in Eq. (26) to provide the necessary corrections.

It should be reemphasized that our result is not in the product form as in Eq. (47) but is a sum of three identical functions with interchange of the  $s, t, u$  variables [Eq. (26) and Eq. (37)]. It is a direct consequence of the fixed  $t$  dispersion relation, using crossing symmetry and neglecting the contribution from higher partial waves at low energy in the absorptive part.

### VII. IMPORTANCE OF THE MULTIPLE SCATTERING CORRECTION AS A FUNCTION OF THE $\rho$ WIDTH

Our formulation of the problem  $\gamma\pi\rightarrow\pi\pi$  is quite useful in understanding the importance of the multiple scattering effects as a function of the  $\rho$  width. We have previously stated that in the large  $N_c$  limit the multiple scattering effects should vanish and we should recover the VMD models as given by Eqs. (10)–(12). In order to see that this statement is correct, it is sufficient to study the correction factor  $J(s)$  defined by Eq. (43) as a function of the  $\rho$  width. It is sufficient to study this question for the case when  $\alpha=0$ . In Fig. 10, the modulus of the function  $J(s)$  is plotted against the energy squared when the  $\rho$  width is increased or decreased by a factor of 4 when  $f_\pi$  is changed by a factor of 2. This can be seen from examining the definition of the function  $\Omega(s)$ , Eq. (16). The result is that the multiple scattering effect increases as the  $\rho$  width increases, and decreases as the  $\rho$  width decreases. It is easy to see that for a zero width resonance the correction factor  $J(s)$  is unity.

The result of this section also provides some arguments for neglect of the multiple scattering effect in the study of  $\langle\gamma|3\pi\rangle$  and  $\langle 3\pi|\pi\gamma\rangle$  with the  $3\pi$  resonating as the  $\omega$  state because of the extremely small width of this resonance [21].

### VIII. CONCLUSION

We have studied in this article the scattering of  $\gamma\pi\rightarrow\pi\pi$  using the integral equation approach. Because the second derivative of the  $P$ -wave amplitude at  $s=m_\pi^2$  is not

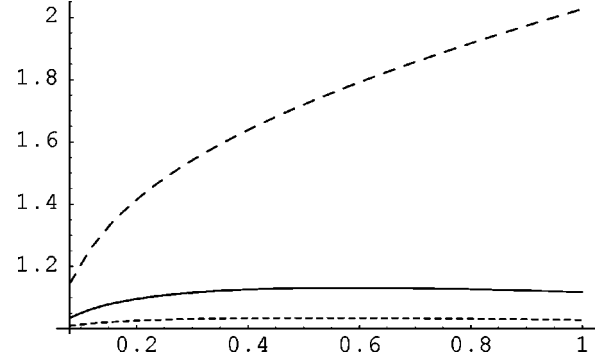


FIG. 10. Plot of the absolute value of  $J(s)$  (vertical axis) defined by Eq. (43) in units of  $\bar{\lambda}$  vs  $s$  ( $\text{GeV}^2$ ) for  $\alpha=0$  for various values of the  $\rho$  width. The solid curve represents  $\Gamma_\rho=0.156$  GeV, the short dashed curve  $\Gamma_\rho=0.039$  GeV, and the long dashed curve  $\Gamma_\rho=0.624$  GeV.

known, the maximum cross section for this process cannot be predicted with reliability. The solution of the integral equation is ambiguous and depends on the second derivative of the  $P$ -wave amplitude at  $s=m_\pi^2$ . This problem is similar to the problem of the contact term in the usual VMD model.

If the ambiguity of the solution of the integral equation can be interpreted as the imperfection of the elastic unitarity relation in describing low energy phenomena, then one must be satisfied with a precision of the order of 15% in amplitude for the pion form factor calculation [4]. This inadequacy can then be removed using knowledge of the pion rms radius [4].

For the  $\gamma\pi\rightarrow\pi\pi$  calculation, this inadequacy becomes more serious because of the existence of singularities associated with the  $t$  and  $u$  channels. Furthermore, the corresponding first derivative of the  $P$ -wave amplitude vanishes because of the symmetry of the problem, and hence we can only use knowledge of the second derivative at  $s=m_\pi^2$  to improve the elastic unitarity relation. This last parameter cannot be precisely measured and hence we cannot predict  $\Gamma(\rho\rightarrow\pi\gamma)$  with certainty.

We show in this article that there is a one-to-one correspondence between the contact term in the VMD model and the ambiguity associated with the parameter  $\alpha$  in our integral equation approach. This parameter plays the role of the second derivative of the  $P$ -wave amplitude at  $s=m_\pi^2$ .

*Note added in proof.* The electromagnetic correction for this process was recently carried out by L.I. Ametler, M. Knecht, and P. Talavera (Ref. [32]). These authors point out that the discrepancy at low energy between the theory and experiment disappears as a consequence of this correction.

### ACKNOWLEDGMENTS

It is a pleasure to thank Torben Hannah for sending me a copy of his paper before publication and for useful discussions. Centre de Physique Théorique is unité propre 014 du CNRS.

- [1] S. L. Adler, Phys. Rev. **177**, 2426 (1969); J. S. Bell and R. Jackiw, Nuovo Cimento A **60**, 47 (1969).
- [2] Particle Data Group, D. Groom *et al.*, Eur. Phys. J. C **3**, 1 (1998).
- [3] S. L. Adler, B. W. Lee, S. B. Treiman, and A. Zee, Phys. Rev. D **4**, 3497 (1971); M. V. Terent'ev, Phys. Lett. **38B**, 419 (1972); J. Wess and B. Zumino, *ibid.* **37B**, 95 (1971); R. Aviv and A. Zee, Phys. Rev. D **5**, 2372 (1972).
- [4] T. N. Truong, hep-ph/0101345.
- [5] Y. M. Antipov *et al.*, Phys. Rev. D **36**, 21 (1987); S. R. Amendolia *et al.*, Phys. Lett. **155B**, 457 (1985).
- [6] S. Rudaz, Phys. Rev. D **10**, 3857 (1974); Phys. Lett. **145B**, 281 (1984); M. T. Terentev, *ibid.* **38B**, 419 (1972); O. Kaymakcalan, S. Rajeev, and J. Schechter, Phys. Rev. D **30**, 594 (1984); T. D. Cohen, Phys. Lett. B **233**, 467 (1989).
- [7] M. Bando, T. Kugo, and K. Yamawaki, Phys. Rep. **164**, 217 (1988); T. Fujiwara, T. Kugo, H. Terao, S. Uehara, and K. Yamawaki, Prog. Theor. Phys. **73**, 926 (1985).
- [8] M. Gell-Mann, D. Sharp, and W. G. Wagner, Phys. Rev. Lett. **8**, 261 (1962).
- [9] J. Bijnens, A. Bramon, and F. Cornet, Phys. Lett. B **237**, 488 (1990).
- [10] B. R. Holstein, Phys. Rev. D **53**, 4099 (1996).
- [11] T. Hannah, Nucl. Phys. **B593**, 577 (2001).
- [12] N. I. Muskhelishvili, *Singular Integral Equations* (Noordhoff, Groningen, 1953); R. Omnés, Nuovo Cimento **8**, 316 (1958).
- [13] M. Gourdin and A. Martin, Nuovo Cimento **16**, 78 (1960); H. S. Wong, Phys. Rev. Lett. **5**, 70 (1960).
- [14] J. J. Sakurai, Ann. Phys. (N.Y.) **11**, 1 (1960); M. Gell-Mann and F. Zachariasen, Phys. Rev. **124**, 953 (1961); Y. Nambu and J. J. Sakurai, Phys. Rev. Lett. **8**, 79 (1962); **8**, 191(E) (1962).
- [15] M. Gell-Mann, D. Sharp, and W. G. Wagner, Phys. Rev. Lett. **8**, 261 (1962).
- [16] G. J. Gounaris and J. J. Sakurai, Phys. Rev. Lett. **21**, 24 (1968).
- [17] K. Kawarabayashi and M. Suzuki, Phys. Rev. Lett. **16**, 255 (1966); Riazuddin and Fayyazuddin, Phys. Rev. **147**, 1071 (1966).
- [18] T. N. Truong, Phys. Rev. Lett. **61**, 2526 (1988).
- [19] K. M. Watson, Phys. Rev. **95**, 228 (1955).
- [20] Le viet Dung and T. N. Truong, hep-ph/9607378.
- [21] T. N. Truong, hep-ph/0102300.
- [22] S. M. Roy, Phys. Lett. **36B**, 353 (1971), J. L. Basdevant, J. C. Le Guillou, and H. Navelet, Nuovo Cimento A **7**, 363 (1972).
- [23] L. Capraro *et al.*, Nucl. Phys. **B288**, 659 (1987).
- [24] J. Huston *et al.*, Phys. Rev. D **33**, 3199 (1986).
- [25] A. M. Bernstein, JLAB Report No. E94-015.
- [26] S. I. Dolinsky, *et al.*, Z. Phys. C **42**, 511 (1989).
- [27] S. D. Protopopescu *et al.*, Phys. Rev. D **7**, 1279 (1973).
- [28] B. Hyams *et al.*, Nucl. Phys. **B64**, 134 (1973).
- [29] P. Eastabrooks and A. D. Martin, Nucl. Phys. **B79**, 801 (1974).
- [30] L. M. Barkov, *et al.*, Nucl. Phys. **B256**, 365 (1985).
- [31] ALEPH Collaboration, R. Barate *et al.*, Z. Phys. C **76**, 15 (1997).
- [32] L.I. Ametler, M. Knecht, and P. Talavera, Phys. Rev. D **64**, 094009 (2001).